

Spectroscopy and dynamics of the dipole-supported state of acetyl fluoride enolate anion

Jeffrey Marks^{a)} and John I. Brauman

Department of Chemistry, Stanford University, Stanford, California 94305

Roy D. Mead,^{b)} Keith R. Lykke, and W. C. Lineberger

Department of Chemistry, University of Colorado and Joint Institute for Laboratory Astrophysics, University of Colorado and National Bureau of Standards, Boulder, Colorado 80309

(Received 30 October 1987; accepted 4 February 1988)

High resolution photodetachment spectroscopy of acetyl fluoride enolate anion has revealed ≈ 200 narrow resonances near the photodetachment threshold, corresponding to excitation of the anion to a diffuse state in which the electron is weakly bound by the field of the molecular dipole. An analysis of the rotational transitions between the ground valence state and the excited dipole-supported state has been carried out, yielding spectroscopic constants for both states. The binding energy of the dipole-supported state is found to be less than 35 cm^{-1} . The dependence of autodetachment lifetimes upon rotational quantum numbers of the dipole-supported state has been measured. The selection rules and dynamics of autodetachment from the dipole-supported state are discussed. The results are compared with those obtained previously for acetaldehyde enolate anion.

I. INTRODUCTION

In negative ions of molecules with large dipole moments it is possible for a diffuse electronic state arising from the dipole–electron interaction to exist. It has been predicted¹ that all molecules with dipole moments greater than $\approx 2 \text{ D}$ should have such a bound state. If the dipole-supported state is an excited state of the negative ion we would expect it to be similar to Rydberg states that are observed in neutral molecules. In Rydberg states² the electron is bound by the Coulomb interaction with the positive core. In the dipole-supported state the electron is bound by dipole–electron interaction.

Several authors have investigated the interaction of an electron with a stationary dipole.³ They found that the minimum dipole moment necessary for a bound state to exist is 1.625 D . Garrett¹ has extended these calculations to include the effects that moment of inertia, dipole length, and rotations have on the magnitude of the critical dipole moment necessary to bind an electron. Other calculations have also examined the possibility of excited states resulting from the dipole–electron interaction.⁴

Recent photodetachment studies of several enolate anions^{5,7} provide strong experimental evidence for the existence of dipole-supported states. It was observed that a number of resonances, corresponding to transitions to a low-lying excited electronic state, occur at the threshold for photodetachment. The excited state does not correspond to any valence transition and has been proposed to be a dipole-supported excited state.⁵ Photodetachment studies on *o*- and *p*-benzoquinone⁶ provide additional evidence of dipole-supported states. Resonances appear in the threshold region for the *o*-benzoquinone negative ion (the dipole moment of the neutral is approximately 5.1 D) but do not appear in the threshold region for the *p*-benzoquinone negative ion (the

neutral has no dipole moment). Both negative ions are stable, with similar electron detachment energies.

In a previous paper⁷ we reported the high resolution photodetachment spectrum of acetaldehyde enolate anion (CH_2CHO^-). By assigning the observed rotational transitions we were able to determine the geometry of the excited and ground states of the anion. It was found that the geometry of the excited state was very similar to that of the radical, consistent with the electron being in a very diffuse molecular orbital. In addition the binding energy of the excited state was found to be only 5 cm^{-1} . A strong dependence of the excited state lifetime on the rotational energy was also observed. The lifetime of the excited state, determined by linewidth measurements, decreased rapidly as the rotational energy increased.

In order to expand our understanding of the detailed nature of dipole-supported excited states, we have obtained the high resolution photodetachment spectrum of acetyl fluoride enolate anion (CH_2COF^-). This system was chosen for study because the anion has a convenient (visible) photodetachment threshold, and the size of the molecule should permit a complete rotational assignment of observed transitions. Acetyl fluoride enolate radical has a large molecular dipole moment ($\approx 3\text{--}5 \text{ D}$), is a near-oblate top, and should possess a dipole-bound state. We find that the binding energy of the dipole-bound state is significantly larger than that of the corresponding state in acetaldehyde enolate, but a little smaller than that in CH_2CN^- . The lifetime of the excited state is observed to be dependent on the rotational quantum numbers of the excited state in addition to the total energy.

II. EXPERIMENTAL

Two sets of experiments are reported in this paper. The first is the 1 cm^{-1} resolution spectrum that was obtained on an ICR spectrometer at Stanford. After interesting features were observed at this resolution, the high resolution spec-

^{a)} Present address: The Aerospace Corporation, P. O. Box 92957, Los Angeles, CA 90009.

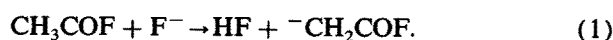
^{b)} Present address: Spectra Technology, Seattle, WA.

trum was obtained on the coaxial ion beam apparatus at Boulder.

A. Ion cyclotron resonance experiments (Stanford)

The 1 cm^{-1} resolution electron photodetachment spectra of acetyl fluoride and acetyl fluoride- d_2 enolates were obtained using an ion cyclotron resonance spectrometer operated in the drift mode.⁸ Typical cell pressures were 1×10^{-7} Torr, with trapping times on the order of 500 ms. Ions were detected using a capacitance bridge equipped with a frequency lock, which has been described in detail elsewhere.⁹

The acetyl fluoride enolate anions were generated by the proton transfer reaction



The primary ion F^- was formed by dissociative electron capture by NF_3 . Deuterated acetyl fluoride was synthesized¹⁰ by reaction of acetic-anhydride- d_6 with benzoyl fluoride followed by distillation of the acetyl fluoride- d_3 .

A Coherent model 590 cw dye laser provided a tunable light source. The wavelength was tuned using a three plate birefringent filter which gave a resolution of 1 cm^{-1} . Rhodamine 110 was used for the entire spectral range covered in these experiments. Dye laser output was 500 mW at the peak of the tuning curve using a 4 W pump from an argon ion laser.

B. Ion beam experiments (Boulder)

The details of this experimental apparatus have been reported in a previous paper.^{7,11} An approximately 2 nA beam of acetyl fluoride enolate ions was generated by extracting the ions from a hot-cathode electric discharge containing 0.1 Torr of acetyl fluoride (CH_3CFO), selecting mass m/e 61 with a 90° sector magnet, and accelerating it to 3 keV. There was also an intense ion at mass m/e 41, corresponding to ketene enolate anion (CHCO^-). The ion beam was then merged with the laser beam over a 30 cm path by means of electrostatic quadrupole deflectors.¹² Acetyl fluoride- d_3 was then used to form the deuterated enolate anion which gave a strong m/e 63 signal.

The laser system used in these experiments was a non-commercial cw dye laser.^{7,13} Two different configurations of the dye laser were used. For broadband low resolution (1 cm^{-1}) spectra the dye laser was operated in a linear configuration and was tuned with a birefringent filter. For single frequency high resolution experiments ($< 20\text{ MHz}$) the laser was operated in a ring configuration. The experiments reported here were carried out using Rhodamine 110 laser dye pumped with 3–4 W of light from an argon ion laser. The dye laser output was 700 mW for broad band operation and 500 mW for single frequency operation.

The line shape of the laser is monitored by two Fabry-Perot etalons. Absolute wavelength calibration (to an accuracy of 0.01 cm^{-1} or $1/4$ of the laser linewidth, whichever is greater) is provided by a lambda-meter¹⁴ (traveling Michelson interferometer) using a polarization-stabilized helium-neon laser reference.¹⁵

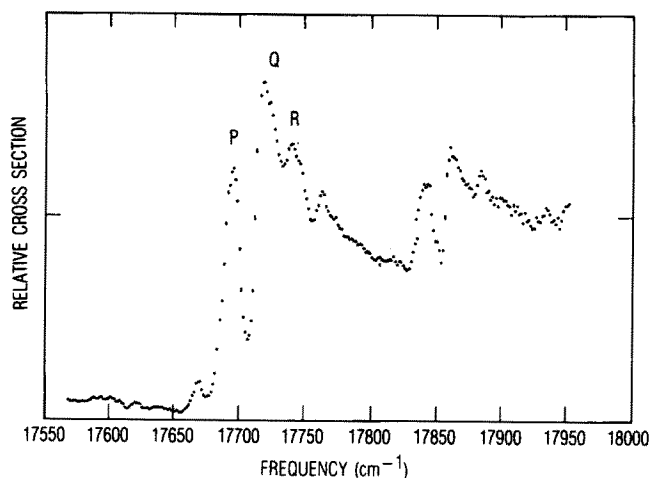


FIG. 1. Relative photodetachment cross section for acetyl fluoride- d_2 enolate, taken at 1 cm^{-1} resolution in the drift ion cyclotron resonance spectrometer.

III. RESULTS

A. Low resolution data

A portion of the 1 cm^{-1} spectra for the acetyl fluoride- d_2 is shown in Fig. 1. A number of prominent resonances are observed in the 1 cm^{-1} resolution spectra of the two enolates. The positions, intensities, and vibrational assignments of these resonances for both the hydrogen and deuterium compounds are given in Table I. The $0 \leftarrow 0$ vibrational transition can be unambiguously assigned by noting that the set of resonances at $17\,704\text{ cm}^{-1}$ does not shift upon deuteration. We would expect the $0 \leftarrow 0$ vibrational band to shift very little, upon deuteration. The shift should be approximately $1/\sqrt{2}$ times the difference in the zero point energies of the ground and excited states with hydrogenic vibrational modes. Hydrogenic vibrational thresholds involving excited

TABLE I. Line positions and intensities of transitions observed in the 1 cm^{-1} resolution spectra.

Line position (cm^{-1})	Vibrational ^a assignment	Intensity
CH₂COF		
17 010	$3a_1^0$	medium
17 229	$3b_1^0$	weak
17 410	4_1^1	medium
17 704	0-0	very strong
17 845	4_1^3	weak
18 104	4_0^2	medium
18 275	$3b_0^1$	very weak
CD₂COF		
17 054	$3a_1^0$	medium
17 285	$3b_1^0$	medium
17 491	4_1^1	medium
17 704	0-0	very strong
17 838	4_1^3	strong
18 047	4_0^2	medium
18 195	$3b_0^1$	very weak

^aMode designations are $\omega_3 = \text{O-C-F}$ deformation; $\omega_4 = \text{CH}_2$ torsion.

levels should shift significantly upon deuteration, and the coincidence of two vibrational transitions in the hydrogen and deuterium compounds would be fortuitous. A similar argument was used in assigning the $0 \leftarrow 0$ transition in acetaldehyde enolate.¹⁶ The less intense bands can then be assigned to be vibrational transitions due to a low frequency torsional mode, and the two O–C–F deformation modes. Our spectra did not extend far enough to observe the C–C or C–O stretching modes.

In a planar molecule, vibrational excitation involving out of plane motion will only be allowed if Δn is even.^{17(a)} The first band to the red of threshold will then correspond to either a $0 \leftarrow 2$ or $1 \leftarrow 1$ transition of the CH_2 torsional mode. Assignment of this band as a $0 \leftarrow 2$ transition would give a vibrational frequency of 147 cm^{-1} for the torsional mode. This would be a 50% decrease in the torsional frequency compared to that of acetaldehyde enolate.^{5,7} Such a large change is not expected, and we therefore assign the band at $17\,410 \text{ cm}^{-1}$ to be the $1 \leftarrow 1$ transition CH_2 torsional mode. Consistent with this assignment, the frequency of this transition is observed to shift by $1/\sqrt{2}$ upon deuteration. A $2 \leftarrow 0$ transition of the CH_2 torsional mode is observed 400 cm^{-1} to the blue of the $0 \leftarrow 0$ transition. Based on this tentative assignment of the $1 \leftarrow 1$ and $2 \leftarrow 0$ transitions we obtain a frequency of 494 cm^{-1} for the torsional frequency in the ground state of the anion. This corresponds to a slightly higher frequency than that observed in acetaldehyde enolate^{5,7} indicating a higher barrier to the torsional motion. A $3 \leftarrow 1$ transition of the CH_2 torsional mode can also be assigned to the band at $17\,845 \text{ cm}^{-1}$. The two bands at $17\,010$ and $17\,229 \text{ cm}^{-1}$ are assigned as the high and low energy $0 \leftarrow 1$ transitions of the two O–C–F deformation modes (ω_{3a} and ω_{3b}).

Each of the vibrational transitions is observed to be composed of a number of smaller resonances. These bands are too closely spaced to be vibrational structure, and we show later that they are the individual rotational branches of the molecule. The vibrational transitions to the blue of threshold are observed to be composed of three distinct bands.

B. High resolution data

The resonances observed in the low resolution spectra can be further resolved into individual rotational transitions. This was accomplished by operating the dye laser in the single frequency mode giving an effective resolution of 90 MHz (0.0031 cm^{-1}), limited by residual Doppler broadening (30 MHz) and the step size in the scan (80 MHz). The transitions^{17(b)} of the Q form Q branch (${}^Q Q: \Delta K_c = 0 \Delta J = 0$) are shown in Fig. 2. Expansions of the sequences observed in the ${}^Q Q$ and ${}^Q P$ transitions are then presented in Figs. 3(a) and 3(b), respectively. These spectra represent an enhancement of 300 in resolution over that shown in Fig. 1.

Acetyl fluoride enolate is a near-oblate asymmetric top. The rotational levels of the ground state and the excited state of the anion are labeled with the conventional J, K_c notation, where J is the total angular momentum and K_c is the projection of J onto the c axis. Even though this molecule is signifi-

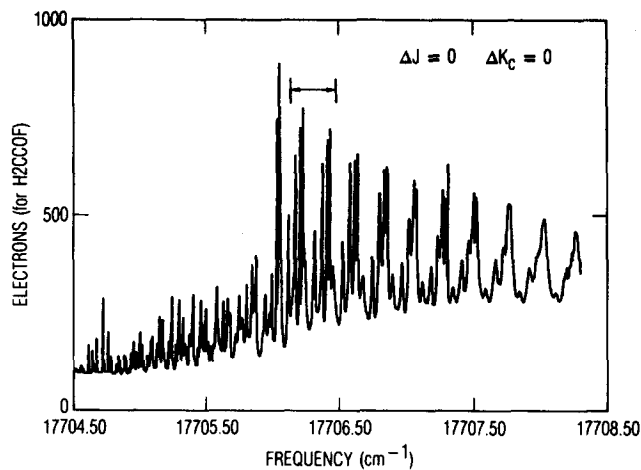


FIG. 2. High resolution (100 MHz or 0.0035 cm^{-1}) neutral cross section spectra of the Q form Q branch ($\Delta K_c = 0, \Delta J = 0$) of the $0 \leftarrow 0$ vibrational transition (frequency is not corrected for the Doppler shift). The rotational transitions are observed to broaden as energy increases. Brackets indicate area expanded in Fig. 3(a).

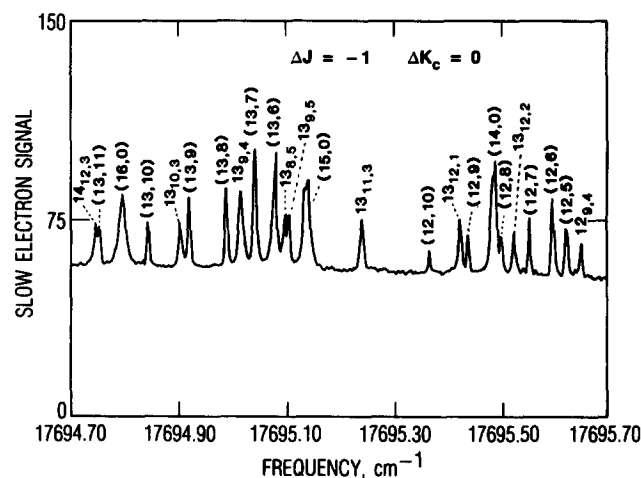
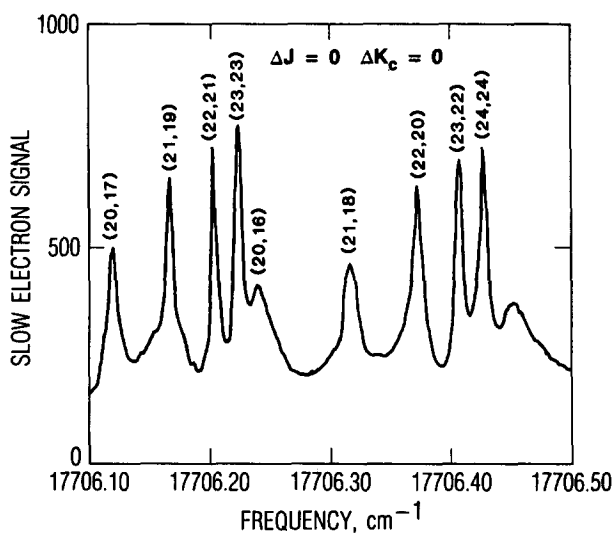


FIG. 3. (a) Individual rotational transitions observed in Q branch. Transitions are labeled JK_c . (b) Rotational transitions observed in P branch. Transitions where asymmetry doubling is resolved are labeled $JK_c K_c$.

cantly asymmetric, for most of the transitions observed in the rotational spectra the value of K_c was sufficiently high^{17(c)} that asymmetry doubling was not resolved. For those transitions where asymmetry doubling was resolved the transitions are labeled with the J, K_a, K_c convention.

The transitions observed in the high resolution spectra correspond to $\Delta J = 0, \pm 1$ and $\Delta K = 0$. Since only transitions with $\Delta K = 0$ are observed, the transition dipole moment must be parallel to the figure axis,^{17(b)} i.e., out of the plane of the molecule. A transition dipole moment out of the plane indicates that the excited and ground states must be of two different representations of the symmetry group of the molecule. Since the anion ground state has A' symmetry, the excited state must have A'' symmetry. The highest occupied molecular orbital (HOMO) of the ground state is a "non-bonding" π orbital. Because the transition moment is out of the plane, and we observe a strong optical transition, the HOMO of the dipole excited state is very likely a σ orbital with a nodal plane perpendicular to the plane of the molecule.

Most of the vibrational structure seen in Fig. 1 is derived from three rotational branches (P, Q, R). In addition to these three branches, weak transitions appear to the red and blue of the 0-0 transition. These may correspond to $\Delta K_c = \pm 2$ transitions, although no high resolution analysis of these bands was attempted.

The rotational assignment was accomplished by noting the presence of two very pronounced patterns in the 2Q and 2P transitions. The pattern observed in the 2Q transitions is

shown in Fig 3(a). It consists of a series of five rotational transitions that become more closely spaced and more intense as the transition energy increases. The sequence then abruptly terminates and a new progression begins. One possible reason for the termination of the sequence would be the last line corresponding to a final state with $J = K_c$. This would also be consistent with the intensity, since in the 2Q transitions the Hönl-London factors are greatest for transitions to states with^{17(d)} $J = K_c$. The other transitions in the sequence then correspond to a decrease in J by 1 and K by 2, moving toward lower energy from the $J = K_c$ line. When J decreases by 1 and K decreases by 2 in a planar oblate top, the rotational energy does not change much. Thus, these groups correspond to a sequence of lines with approximately the same rotational energy, as would be expected for transitions in the Q branch. In Fig. 3(b), the pattern observed in the P branch is shown. Here the sequence is composed of transitions all ending in the same final J state and forming a progression with decreasing values of K as the transition energy increases. The assignment and line positions of the observed rotational transitions are given in Table II.

The line position and assignment of the observed transitions were entered into a nonlinear least-squares program¹⁸ which fit the data to seven parameters: the band origin and the rotational constants $A, B,$ and C for the ground and excited states. The energy levels for a symmetric oblate rotor ($A = B > C$) are^{17(e)} given by $E_{J,K} = J(J+1)B - K^2(B - C)$. Since $B > C$, the energy of the rotational levels decreases as K increases. The rotational energy levels for this

TABLE II. The observed line positions corrected for the Doppler shift, and Δ the difference between the calculated and measured line positions, for the Q branch and P branch rotational transitions.

Final state ^a JK_c	Initial state JK_c	Observed frequency (cm^{-1})	Δ (cm^{-1})	Final state ^a JK_c	Initial state JK_c	Observed frequency (cm^{-1})	Δ (cm^{-1})
Q form Q branch							
10 6	10 6	17 710.366	0.007	16 15	16 15	17 710.941	-0.004
11 9	11 9	17 710.373	0.007	17 17	17 17	17 710.960	-0.003
10 5	10 5	17 710.399	0.008	15 12	15 12	17 710.996	0.001
12 11	12 11	17 710.407	0.009	14 9	14 9	17 710.996	0.000
13 13	13 13	17 710.423	0.012	14 8	14 8	17 711.053	0.002
11 8	11 8	17 710.433	0.012	16 14	16 14	17 711.053	-0.003
11 7	11 7	17 710.494	0.006	15 11	15 11	17 711.082	0.003
12 10	12 10	17 710.494	0.004	17 16	17 16	17 711.086	0.001
13 12	13 12	17 710.531	0.003	14 7	14 7	17 711.096	0.005
11 6	11 6	17 710.542	0.001	18 18	18 18	17 711.104	0.003
14 14	14 14	17 710.549	0.004	16 13	16 13	17 711.157	-0.001
12 9	12 9	17 710.570	0.001	17 15	17 15	17 711.215	-0.003
13 11	13 11	17 710.616	0.008	15 9	15 9	17 711.231	0.000
12 8	12 8	17 710.628	0.006	18 17	18 17	17 711.251	-0.005
14 13	14 13	17 710.675	-0.015	16 12	16 12	17 711.254	0.001
12 7	12 7	17 710.691	-0.005	19 19	19 19	17 711.270	-0.004
15 15	15 15	17 710.702	-0.022	17 14	17 14	17 711.328	-0.006
13 10	13 10	17 710.715	-0.010	18 16	18 16	17 711.383	-0.007
14 12	14 12	17 710.744	0.014	19 18	19 18	17 711.415	-0.002
13 9	13 9	17 710.758	0.018	20 20	20 20	17 711.433	0.000
15 14	15 14	17 710.777	0.017	18 15	18 15	17 711.499	-0.002
16 16	16 16	17 710.802	0.012	19 17	19 17	17 711.554	-0.003
13 8	13 8	17 710.825	0.013	20 19	20 19	17 711.594	-0.006
14 11	14 11	17 710.836	0.011	21 21	21 21	17 711.610	-0.001
13 7	13 7	17 710.886	0.001	19 16	19 16	17 711.694	-0.014
15 13	15 13	17 710.899	0.001	20 18	20 18	17 711.742	-0.008
14 10	14 10	17 710.925	0.002	21 20	21 20	17 711.779	-0.008

TABLE II (continued).

Final state ^a JK_c	Initial state JK_c	Observed frequency (cm^{-1})	Δ (cm^{-1})	Final state ^a JK_c	Initial state JK_c	Observed frequency (cm^{-1})	Δ (cm^{-1})
22 22	22 22	17 711.796	-0.004	16 12	17 12	17 698.972	-0.008
20 17	20 17	17 711.867	0.003	16 11	17 11	17 699.057	-0.006
21 19	21 19	17 711.915	0.010	16 10	17 10	17 699.133	-0.004
22 21	22 21	17 711.952	0.011	16 9	17 9	17 699.195	0.000
23 23	23 23	17 711.973	0.011	16 8	17 8	17 699.249	0.000
20 16	20 16	17 711.989	0.010	16 7	17 7	17 699.283	0.005
21 18	21 18	17 712.065	0.005	16 6	17 6	17 699.304	0.005
22 20	22 20	17 712.120	0.004	15 13	16 13	17 699.339	-0.004
23 22	23 22	17 712.157	0.005	15 12	16 12	17 699.437	-0.005
24 24	24 24	17 712.178	0.006	15 11	16 11	17 699.517	0.004
21 17	21 17	17 712.204	0.002	15 10	16 10	17 699.594	0.005
22 19	22 19	17 712.278	-0.001	15 9	16 9	17 699.660	0.008
23 21	23 21	17 712.331	0.001	15 8	16 8	17 699.722	0.004
24 23	24 23	17 712.365	0.005	15 7	16 7	17 699.768	0.002
25 25	25 25	17 712.386	0.005	15 6	16 6	17 699.798	-0.001
22 18	22 18	17 712.425	-0.004	15 _{11 5}	16 _{12 5}	17 699.814	-0.001
23 20	23 20	17 712.496	-0.004	15 _{12 4}	16 _{13 4}	17 699.858	0.013
24 22	24 22	17 712.552	-0.004	15 _{11 4}	16 _{12 4}	17 699.622	-0.003
25 24	25 24	17 712.584	0.001	15 0	16 0	17 700.885	-0.004
26 26	26 26	17 712.606	0.002	14 12	15 12	17 699.910	0.005
23 19	23 19	17 712.646	-0.002	14 11	15 11	17 700.000	0.005
24 21	24 21	17 712.721	-0.004	14 10	15 10	17 700.075	0.010
25 23	25 23	17 712.776	-0.004	14 9	15 9	17 700.145	0.011
26 25	26 25	17 712.811	0.000	14 8	15 8	17 700.207	0.009
27 27	27 27	17 712.826	0.006	14 7	15 7	17 700.260	0.004
		<i>Q</i> form <i>P</i> branch		14 6	15 6	17 700.296	0.001
22 22	23 22	17 695.167	-0.001	14 _{10 5}	15 _{11 5}	17 700.313	0.003
22 21	23 21	17 695.336	0.000	14 _{11 4}	15 _{12 4}	17 700.363	-0.005
22 20	23 20	17 695.493	0.006	14 _{12 3}	15 _{13 3}	17 700.494	0.021
22 19	23 19	17 695.652	0.000	14 0	15 0	17 701.234	-0.005
21 21	22 21	17 695.703	0.002	13 11	14 11	17 700.500	0.004
21 20	22 20	17 695.862	0.006	13 10	14 10	17 700.587	-0.001
21 19	22 19	17 696.020	0.002	13 9	14 9	17 700.667	-0.008
21 18	22 18	17 696.168	0.000	13 8	14 8	17 700.733	-0.012
21 17	22 17	17 696.303	0.001	13 7	14 7	17 700.785	-0.012
20 20	21 20	17 696.252	0.001	13 6	14 6	17 700.825	-0.015
20 19	21 19	17 696.406	0.002	13 ₅	14 _{10 5}	17 700.854	-0.019
20 18	21 18	17 696.554	-0.001	13 _{8 5}	14 _{9 5}	17 700.841	-0.018
20 17	21 17	17 696.698	-0.007	13 _{10 4}	14 _{11 4}	17 700.881	-0.015
19 19	20 19	17 696.817	-0.009	13 _{9 4}	14 _{10 4}	17 700.762	-0.001
19 18	20 18	17 696.959	-0.004	13 _{11 3}	14 _{12 3}	17 700.987	-0.004
19 17	20 17	17 697.108	-0.015	13 _{10 3}	14 _{11 3}	17 700.648	-0.006
19 16	20 16	17 697.231	-0.008	13 _{12 2}	14 _{13 2}	17 701.267	-0.021
19 15	20 15	17 697.355	-0.011	13 _{12 1}	14 _{13 1}	17 701.167	0.025
18 18	19 18	17 697.381	-0.008	13 0	14 0	17 701.600	0.003
18 17	19 17	17 697.514	-0.002	12 10	13 10	17 701.108	-0.006
18 16	19 16	17 697.642	0.000	12 9	13 9	17 701.182	-0.007
18 15	19 15	17 697.763	0.000	12 8	13 8	17 701.244	-0.005
18 14	19 14	17 697.865	0.010	12 7	13 7	17 701.295	-0.002
18 13	19 13	17 697.971	0.008	12 6	13 6	17 701.338	-0.003
18 12	19 12	17 698.061	0.012	12 5	13 5	17 701.367	-0.003
17 17	18 17	17 697.934	0.010	12 _{9 4}	13 _{10 4}	17 701.396	-0.006
17 16	18 16	17 698.073	0.003	12 _{10 3}	13 _{11 3}	17 701.471	0.006
17 15	18 15	17 698.196	0.002	11 8	12 8	17 701.764	0.008
17 14	18 14	17 698.309	0.002	11 7	12 7	17 701.819	0.009
16 14	17 14	17 698.768	-0.006	11 6	12 6	17 701.870	0.003
16 13	17 13	17 698.883	-0.015				

^aStates where individual asymmetry components occur are labeled J_{KaKc} .

system (a near-oblate top) are shown in Fig. 4. The energy levels of an asymmetric top can be calculated using a perturbation expansion,^{17(f),19} or by expanding the asymmetric top wave function in an oblate top basis²⁰ and diagonalizing the matrix containing the interaction between states of different

K_c for a given J . Energies were computed using the matrix method.²⁰ The rotational constants obtained from the fit are given in Table III with their associated error limits. The standard deviation of the residuals is approximately equal to the 0.01 cm^{-1} random error in wavelength measurement.

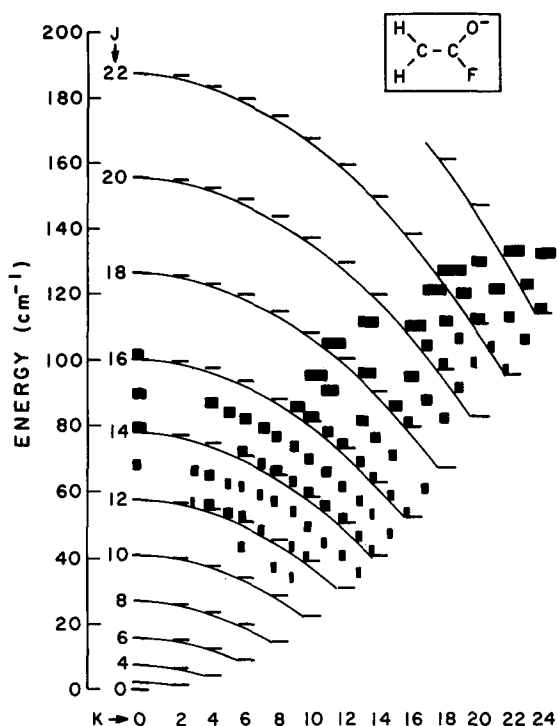


FIG. 4. Energy level diagram of the dipole-supported excited state. The relative linewidth of the transitions is indicated by the width of the bars.

All of the 169 lines for which a precise position could be measured were included in the fit.

For parallel-type transitions it is necessary to assign some of the asymmetry states in order to obtain a unique set of rotational constants.^{17(g)} In the high energy end of the *P* branch it was possible to assign these asymmetry doublets, allowing a unique fit to be achieved. The small positive value of the inertial defect, obtained from $\Delta = I_c - I_a - I_b$, is indicative of the possible planarity of the molecule. Using the rotational constants obtained from fitting the data we find that both the excited and ground states appear to be planar (small positive inertial defect) to within the experimental

TABLE III. Rotational constants obtained from least-squares fitting of data in Table II.

Constant	(cm ⁻¹) ^a
<i>A</i> '	0.381 85 (7)
<i>B</i> '	0.357 69 (7)
<i>C</i> '	0.184 3 (2)
Δ ' ^b	0.19 (19)
<i>A</i> "	0.368 30 (7)
<i>B</i> "	0.354 64 (7)
<i>C</i> "	0.180 2 (2)
Δ " ^b	0.24 (19)
ν_0	17 709.646 (3)
σ^d	0.007

^a Values in parentheses are one standard error.

^b Δ is the inertial defect $I_c - I_a + I_b$, in amu Å².

^c This number is the Doppler corrected value, whereas the figures show the uncorrected numbers.

^d Standard deviation of fit.

error of our measurements. The high resolution spectrum of the 2R transitions was not recorded.

We also recorded the high resolution spectrum of the deuterated acetyl fluoride enolate anion. Because of the high density of lines we were unable to identify the $J = K_c$ transition in the *Q* branch. Thus, individual patterns could not be identified, and it was not possible for us to make an assignment of the transitions observed in this ion.

C. Molecular structure

In acetaldehyde enolate it was observed that the structure of the excited state was very similar to that of the neutral radical.⁷ The C–C bond length was found to increase, and the C–O bond length to decrease upon excitation to the dipole state. The change in the C–C bond upon excitation was greater than the change in the C–O bond length. Thus, we could consider the excited state of acetaldehyde enolate to be looser than the ground state. The structure of acetyl fluoride enolate is shown in Fig. 5. The *c* axis in this ion lies close to the central carbon. The rotational constant *C* therefore reflects primarily the bond lengths of the atoms attached to the central carbon. In acetyl fluoride there is a strong correlation between the C–O, C–C and C–F bonds with respect to the value of the rotational constant *C*. Because we studied only one isotopic species and because of this strong correlation, it was not possible to determine the geometry of the excited and ground states of the anion. In this anion the rotational constant *C* increases upon excitation to the dipole state, indicating that the excited state is tighter than the ground state. This result is indicative of some antibonding character in the ground state of the anion. This antibonding character is removed upon excitation of the electron to a diffuse nonbonding orbital in the dipole state, thus causing the dipole state to tighten up. It is quite possible that in the excited state the C–C bond lengthens and the C–O bond shortens, in accord with expected changes in bond order on going from the strongly resonance stabilized enolate anion to the weakly stabilized radical.

Since the rotational constants of acetyl fluoride enolate radical have not been measured, we cannot determine how closely the dipole state resembles the neutral radical. We believe, however, that the molecular structure of the dipole state is similar to that of the radical.

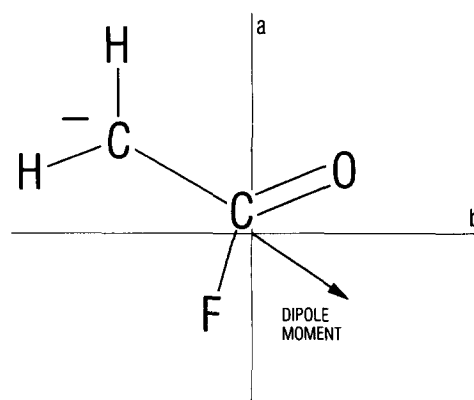


FIG. 5. Structure of acetyl fluoride enolate anion showing orientation with respect to the principal axes.

D. Binding energy

Autodetachment will only be observed from rotational levels that are higher in energy than the binding energy of the excited state. An upper limit to the binding energy can be found by noting that a number of transitions are not observed in the high resolution spectra. The lack of these transitions can be attributed to these states of the anion being bound. Thus, by determining which transitions are not observed and at what excited state energy transitions are first observed we can find the upper limit to the binding energy. The energies of a number of observed transitions are shown in Fig. 4. Since the lowest energy final state we can detect has $J = 12$ and $K_c = 10$, we know that the maximum binding energy is 35 cm^{-1} . As the final state energy approaches the binding energy, an excited state may actually be unbound but autodetach too slowly to be very intense, as has been found in other systems.²¹⁻²³ Thus, it is difficult to determine if the transitions do not occur or are just very weak.

E. Excited state lifetimes

The individual rotational transitions observed in the spectra of acetyl fluoride enolate are found to have linewidths that are dependent on the rotational quantum numbers of the excited state. We observed in acetaldehyde enolate that the lifetime of the excited state decreased very rapidly with increasing rotational energy. Results from a recent photodetachment study of the conjugate base of acetonitrile²¹ indicated that the lifetime of the dipole-supported state was also sensitive to rotations. A strong dependence of the excited state lifetime upon rotational quantum numbers has also been observed²⁴ in NH^- . (This is not a dipole-supported excited state.) In NH^- the lifetime was found to depend on the total rotational energy and on selection rules governing the autodetachment process.

In acetyl fluoride enolate the dipole moment does not lie along any of the principle moments of inertia, so that any rotation will also rotate the dipole moment. We find that overall the lifetime of the excited state decreases as the rotational energy increases, although over small regions some higher energy states actually autodetach more slowly. In the 2Q transitions shown in Fig. 3(a), the energy of the final state $J = 24$ $K_c = 24$ is higher by 7 cm^{-1} than the state $J = 21$ $K_c = 18$. However, the transition to the lower energy state is twice as broad as the transition to the higher level (see Fig. 4). These results can be best understood by considering the possible autodetachment channels for the excited state.

The lifetime of the excited state will be determined by how well the excited state couples to the final ($e^- +$ neutral radical) states. Any autodetachment channel must of course conserve angular momentum and energy. If the excited state is strongly bound electronically, a large change in angular momentum might be required to provide the minimum energy needed for autodetachment of the anion, thus causing the excited state to be long lived. An energy level diagram of the anion excited state is shown in Fig. 4. The rotational levels of the neutral radical can be estimated by assuming the same rotational constants as the excited state, and then offsetting

the energy by the 35 cm^{-1} bound obtained earlier. Using such a diagram, and looking for the highest J value in the radical that is still lower in energy than the state which is autodetaching, we find that for autodetachment to occur from excited states with rotational quantum numbers $J = K_c$, the dipole state must undergo a change of at least $\Delta J = 4$ or 5 upon autodetachment, requiring the electron to leave as a g or h wave. For states with similar energy and $J > K_c$, the electron can leave as a d or even p wave. Because there is a large angular momentum barrier for the electron leaving as a g wave, and because a large transfer of angular momentum from molecular rotation to orbital angular momentum is expected to be inefficient, the former transition is slower than the transitions in which the electron can leave as a d or p wave. A plot of linewidth vs ΔJ for a number of transitions with approximately the same rotational energy is given in Fig. 6. From this plot we see that the lifetime of the excited state increases, as the minimum change in angular momentum required for autodetachment increases.

In acetaldehyde enolate the lifetime of the excited state decreases with increasing rotational energy much more rapidly than it does in acetyl fluoride enolate. We are able to observe transitions that are over 100 cm^{-1} above the binding energy, compared to transitions becoming too broad to identify within 20 cm^{-1} of the binding energy in acetaldehyde. There are two possible reasons for this decrease in the sensitivity of the lifetime to rotational energy. The first is that because of the larger binding energy, the transitions are simply slower because of larger angular momentum barriers due to large changes in J upon autodetachment. This argument is not sufficient to explain the results, because we are able to observe transitions to final states ($J = 18$ $K_c = 11$) that can autodetach via a p or s wave, yet are still 50 cm^{-1} above the binding energy and not too broad to be observed. The other explanation is that because of an increase in the

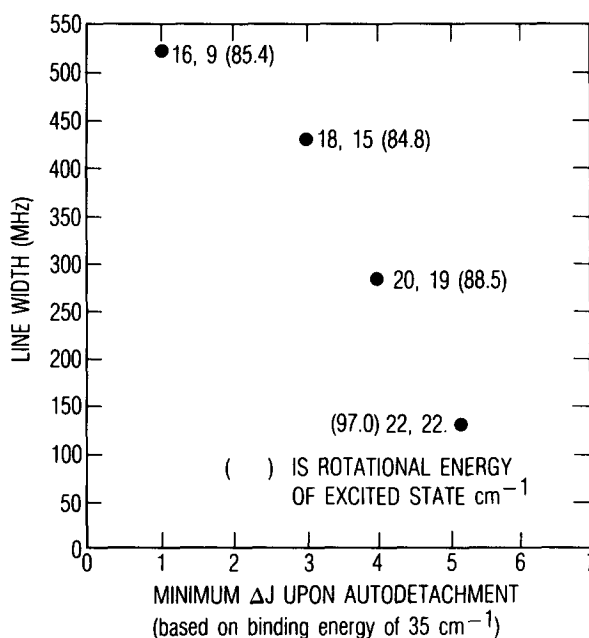


FIG. 6. Linewidth vs minimum required ΔJ for electron autodetachment. The final states all have similar rotational energy.

electron–dipole interaction, the dipole–electron binding becomes less sensitive to rotations. This interaction was investigated for a simple rotating dipole by Garrett,¹ who found that larger dipole moments bind many more rotational levels. More complex calculations will be necessary to investigate this effect in molecules. The increase in the binding energy of the acetyl fluoride enolate compared to the acetaldehyde is probably due to a larger molecular dipole moment.

IV. CONCLUSION

The high resolution photodetachment spectrum of acetyl fluoride enolate has been measured, and we have found the existence of a nonconventional electronic state arising from a dipole–electron interaction. The binding energy is found to be less than 35 cm^{-1} , which is considerably larger than the maximum binding energy (5 cm^{-1}) found for the dipole-supported state in acetaldehyde enolate. The increase in the binding energy is attributed to a larger molecular dipole moment in acetyl fluoride enolate radical. The lifetime of the excited state decreases as the rotational energy of the ion increases, and the change in angular momentum upon autodetachment is shown to have an important role in determining the lifetime. In addition, the change in the rotational constants between the excited and ground states of the anion indicate that the dipole-supported state has shorter bond lengths than does the ground state.

Since the rotational constants of the acetyl fluoride radical are not known we cannot determine how similar the dipole state is structurally to the radical. Additional studies of dipole-supported states should provide insight into the mechanisms for electron autodetachment and bonding in molecular anions.

Note added in proof: For some recent theoretical insights into dipole-bound and dipole-supported states, see D. C. Clary, *J. Phys. Chem.* (in press).

ACKNOWLEDGMENTS

We thank J. L. Hall and L. Hollberg for help with the design and construction of the laser system. C. V. Kunasz and J. Levine provided valuable computational assistance. We are grateful to J. Simons, P. B. Comita, and D. M. Wetzel for helpful discussions. J. Marks acknowledges the support

of an Exxon graduate fellowship. Support for this research was provided by the National Science Foundation under Grant Nos. CHE83-16628, PHY86-04504, and CHE86-11260.

- ¹W. R. Garrett, *Chem. Phys. Lett.* **5**, 393 (1970); *Phys. Rev. A* **3**, 961 (1971).
- ²J. I. Steinfeld, *Molecules and Radiation* (MIT, Cambridge, 1978), p. 214.
- ³(a) E. Fermi and E. Teller, *Phys. Rev.* **72**, 406 (1947); (b) R. F. Wallis, R. Herman, and H. Milnes, *J. Mol. Spectrosc.* **4**, 51 (1960); (c) M. H. Mittleman and V. P. Myerscough, *Phys. Lett.* **23**, 545 (1966); (d) O. H. Crawford, *Proc. Phys. Soc. London* **91**, 279 (1967); (e) for an excellent and entertaining review see J. E. Turner, *Am. J. Phys.* **45**, 758 (1977).
- ⁴(a) W. R. Garrett, *J. Chem. Phys.* **73**, 5721 (1980); (b) **77**, 3666 (1982).
- ⁵R. L. Jackson, A. H. Zimmerman, and J. I. Brauman, *J. Chem. Phys.* **71**,
- ⁶J. Marks, P. B. Comita, and J. I. Brauman, *J. Am. Chem. Soc.* **107**, 3718 (1985).
- ⁷K. R. Lykke, R. D. Mead, and W. C. Lineberger, *Phys. Rev. Lett.* **52**, 2221 (1984); R. D. Mead, K. R. Lykke, W. C. Lineberger, J. Marks, and J. I. Brauman, *J. Chem. Phys.* **81**, 4883 (1984).
- ⁸K. C. Smyth and J. I. Brauman, *J. Chem. Phys.* **56**, 1132 (1972).
- ⁹J. Marks, P. S. Drzaic, R. F. Foster, D. M. Wetzel, J. I. Brauman, J. S. Uppal, and R. H. Staley, *Rev. Sci. Instrum.* **58**, 1460 (1987).
- ¹⁰G. A. Olah, S. J. Kuhn, W. S. Tolgyesi, and E. B. Baker, *J. Am. Chem. Soc.* **84**, 2733 (1962).
- ¹¹U. Hefter, R. D. Mead, P. A. Schulz, and W. C. Lineberger, *Phys. Rev. A* **22**, 1429 (1983).
- ¹²H. D. Zeman, *Rev. Sci. Instrum.* **48**, 1079 (1977).
- ¹³L. Hollberg and J. L. Hall (personal communication).
- ¹⁴S. A. Lee and J. L. Hall, *Appl. Phys. Lett.* **25**, 367 (1976).
- ¹⁵R. Balhorn, H. Kunzmann, and F. Lebowsky, *Appl. Opt.* **11**, 742 (1972).
- ¹⁶R. L. Jackson, P. C. Hiberty, and J. I. Brauman, *J. Chem. Phys.* **74**, 3705 (1981).
- ¹⁷G. Herzberg, *Electronic Spectra of Polyatomic Molecules* (Van Nostrand, New York, 1967): (a) p. 151; (b) p. 222; (c) p. 108; (d) p. 226; (e) p. 84; (f) p. 106; (g) p. 250.
- ¹⁸C. Kunasz, program NLHOUS (personal communication).
- ¹⁹S. R. Polo, *Can. J. Phys.* **35**, 880 (1957).
- ²⁰G. W. King, R. M. Hainer, and P. C. Cross, *J. Chem. Phys.* **11**, 27 (1943).
- ²¹K. R. Lykke, D. M. Neumark, T. Andersen, V. Trapa, and W. C. Lineberger, in *Laser Spectroscopy VII*, edited by Y. R. Shen and T. W. Hansch (Springer, Berlin, to be published); J. Marks, D. M. Wetzel, P. B. Comita, and J. I. Brauman, *J. Chem. Phys.* **84**, 5284 (1986); K. R. Lykke, D. M. Neumark, T. Andersen, V. Trapa, and W. C. Lineberger, *ibid.* (in press).
- ²²K. K. Murray, K. R. Lykke, and W. C. Lineberger, *Phys. Rev. A* **36**, 699 (1987).
- ²³T. Andersen, K. R. Lykke, D. M. Neumark, and W. C. Lineberger, *J. Chem. Phys.* **86**, 1858 (1987).
- ²⁴D. M. Neumark, K. R. Lykke, T. Andersen, and W. C. Lineberger, *J. Chem. Phys.* **83**, 4364 (1985).